II)-Ru(III) ions involves π^* levels based on the Ru-O-Ru bridge and the added proton stabilizes the electron-rich Ru-O-Ru group.

Acknowledgments are made to the National Science Foundation under Grant No CHE-8601604 and the National Institutes of Health under Grant No GM32296 for support of this research. A.L. acknowledges fellowship support from Fulbright "La Caixa" (Barcelona, Spain). P.D. acknowledges the Centre Nationale de la Recherche Scientific (CNRS), France, for financial support.

Registry No. *trans*-[(trpy)(pic)RuCl], 111958-91-9; *cis*-[(trpy)(pic)RuCl], 112019-21-3; *trans*-[[(trpy)(pic)Ru]$_2$O](ClO$_4$)$_2$, 111959-06-9; *cis*-[[(trpy)(pic)Ru]$_2$O](ClO$_4$)$_2$, 112019-23-5; [(tmp)(bpy)RuCl]Cl, 111975-11-2; [(tmp)(phen)RuCl]Cl, 111958-92-0; [(tmp)(4,4'-(CH$_3$)$_2$-bpy)RuCl]Cl, 111975-12-3; *trans*-[(trpy)(pic)Ru(H$_2$O)](ClO$_4$), 111959-09-2; *cis*-[(trpy)(pic)Ru(H$_2$O)](ClO$_4$), 112065-87-9; [(tpm)(bpy)Ru(H$_2$O)](ClO$_4$)$_2$, 111958-94-2; [(tpm)(phen)Ru(H$_2$O)](ClO$_4$)$_2$, 111958-96-4; [(tpm)(4,4'-(CH$_3$)$_2$-bpy)Ru(H$_2$O)](ClO$_4$)$_2$, 111958-98-6; *trans*-[(trpy)(pic)Ru(H$_2$O)]$^{3+}$, 111959-10-5; *cis*-[(trpy)(pic)Ru(H$_2$O)]$^{3+}$, 112019-25-7; [(tpm)(bpy)Ru(H$_2$O)]$^{4+}$, 111958-99-7; [(tpm)(phen)Ru(H$_2$O)]$^{4+}$, 111975-13-4; [(tpm)(4,4'-(CH$_3$)$_2$-bpy)Ru(H$_2$O)]$^{4+}$, 111959-00-3; *trans*-[(trpy)(pic)Ru(H$_2$O)]$^{2+}$, 112065-80-2; *cis*-[(trpy)(pic)Ru(H$_2$O)]$^{2+}$, 111959-11-6; [(tpm)(bpy)Ru(H$_2$O)]$^{3+}$, 111959-01-4; [(tpm)(phen)Ru(H$_2$O)]$^{3+}$, 111959-02-5; [(tpm)(4,4'-(CH$_3$)$_2$-bpy)Ru(H$_2$O)]$^{3+}$, 111959-03-6; [(trpy)RuCl$_3$], 72905-30-7; [(tpm)RuCl$_3$], 111975-10-1; *trans*-[(trpy)(pic)Ru^{III}-O-Ru^{IV}(pic)(trpy)]$^{3+}$, 111959-04-7; *cis*-[(trpy)(pic)Ru^{III}-O-Ru^{IV}(pic)(trpy)]$^{3+}$, 112019-24-6; *trans*-[(trpy)(pic)Ru^{II}-OH-Ru^{IV}(pic)(trpy)]$^{+}$, 112065-85-7; *cis*-[(trpy)(pic)-Ru^{II}-OH-Ru^{II}(pic)(trpy)]$^{+}$, 111959-07-0.

Supplementary Material Available: Figure S1 (UV-visible spectra of *cis*-[(trpy)(pic)Ru^{II}(H$_2$O)]$^{+}$ (---) and electrochemically generated *cis*-[(trpy)(pic)Ru^{III}(OH)]$^{+}$ (···) at pH 7), Figure S2 (cyclic voltammograms of (A) *trans*-[(trpy)(pic)Ru^{II}(H$_2$O)](ClO$_4$) at pH 7, (B) *trans*-[(trpy)(pic)Ru^{IV}(O)](ClO$_4$) at pH 3, and (C) *cis*-[(trpy)(pic)Ru^{II}-(H$_2$O)](ClO$_4$) at pH 7 (0.1 M phosphate buffers, scan rate 50 mV/s)), Figure S3 (cyclic voltammograms of *trans*- and *cis*-[[(trpy)(pic)-Ru]$_2$O](ClO$_4$)$_2$ vs SSCE in water at pH 6.5 (0.1 M phosphate buffer, scan rate 50 mV/s)), and Figure S4 (^{1}H NMR spectra of [(tpm)(b)-Ru(H$_2$O)](ClO$_4$)$_2$ in D$_2$O, where (A) b = bpy and (B) b = 4,4'-(CH$_3$)$_2$-bpy) (4 pages). Ordering information is given on any current masthead page.

Contribution from the Department of Chemistry, National Taiwan University, Taipei, Taiwan, Republic of China, and Department of Crystallography and Mineralogy, University of Frankfurt, Frankfurt, West Germany

Experimental Charge Density Study of 1,3-Dithietane 1,1,3,3-Tetraoxide, $(CH_2SO_2)_2$

Yu Wang,*† L. W. Guo,† H. C. Lin,† C. T. Kao,† C. J. Tsai,† and J. W. Bats‡

Received June 1, 1987

A single crystal of 1,3-dithietane 1,1,3,3-tetraoxide, $(CH_2SO_2)_2$, has been studied by X-ray diffraction at 300 and 104 K. It crystallizes in the monoclinic space group $P2_1/n$, with cell parameters a = 5.527 (2) Å, b = 5.709 (2) Å, c = 8.042 (3) Å, and β = 100.89 (3)° at 104 K; Z = 2. The molecule has a four-membered S-C-S-C ring with the center of the ring at $\bar{1}$. There is a short S-S across the ring distance of 2.593 Å. A bonding electron density study was performed with the 104 K data. The X-X deformation map of the four-membered ring shows a significant amount of density around sulfur atom. There is a peak of 0.57 e Å^{-3} in the S-C bond, polarized toward the sulfur atom. The $-SO_2$ and $-CH_2$ planes are nearly perpendicular to the four-membered ring. The accumulation of electron density in the S-O bond is at the center of the bond, comparable with a recent MO calculation. Such comparison led to the experimental proof of the important role of polarization basis sets including d functions of the sulfur atom in the theoretical bonding electron density studies.

Introduction

$(CH_2SO_2)_2$ has been studied by X-ray diffraction at room temperature both in this laboratory and quite independently by Balback et al. in 1980.[1] The crystal is very stable and yields good diffraction intensity measurements. The crystal was chosen to investigate its bonding electron density distribution at low temperature. This molecule is particularly interesting in its small ring structure and its short S-S contact distance. The questions we would like to answer in this study are as follows: First, does the four-membered ring structure suffer from ring strain? Second, is there any contribution in charge density distribution from the d functions of the sulfur atom? Third, what is the character of the S-O bond? Finally, is there any interaction between sulfur atoms across the ring?

Experimental Section

The title compound was prepared by reacting CH_2SO_2Cl with trimethylamine in THF at -20 °C.[2] The suitable colorless single crystals for diffraction studies were obtained by diffusing ethanol into a saturated DMF solution.

The crystal data of $(CH_2SO_2)_2$ at both 300 and 104 K are listed in Table I. The intensity data at both temperatures were collected with CAD4 diffractometer equipped with a graphite monochromator and liquid N_2 gas flow set up. The experimental details are also given in Table I. The intensity data at 104 K were measured up to 2θ of 110°, two (three in some cases) more equivalent reflections were measured up to 86°. Beyond 110°, only 80 calculated strong reflections were measured. These yield a total of 8725 measurements, which gave 3273 unique reflections after averaging of equivalents. A 14% linear decay of

Table I. Crystal Data for $(CH_2SO_2)_2$ at 300 and 104 K

	300 K	104 K
formula	$(CH_2SO_2)_2$	
mol wt	156.17	
cryst size, mm	0.3 × 0.3 × 0.5	0.24 × 0.14 × 0.24
space group	$P2_1/n$	$P2_1/n$
a, Å	5.587 (2)	5.527 (2)
b, Å	5.757 (3)	5.709 (2)
c, Å	8.125 (2)	8.042 (3)
β, deg	100.89 (2)	100.89 (3)
V, Å^3	256.63	249.21
Z	2	2
D_{calcd}, g/cm^3	2.021	2.081
F_{000}	160	160
radiation	Mo Kα (λ = 0.7107 Å)	Mo Kα
scan speed, deg/min	20/3	20/3-20/16
2θ range (Mo Kα), deg	4-54	5-128.1
$\theta/2\theta$ scan param	2(1.0 + 0.35 tan θ)	2(0.95 + 0.5 tan θ)
abs coeff, cm^{-1}	9.4	9.4
transmittance factor		0.79-0.89
total no. of reflcns	682	3273
no. of obsd rflcns (>2σ)	494	3068
$\sum_i I_i - \langle I \rangle / \sum_i I_i$		0.013
quadrant collcd	$h,k,\pm l$	$h,k,\pm l$; $h,-k,\pm l$; additional $-h,\mp k,\pm l$
R, R_w	0.033, 0.028	0.030, 0.027
S	2.43	1.51
f ($W(f) = 1/[\sigma_c^2(F_o) + fF_o^2]$)	0	0.000 07

* To whom correspondence should be addressed.
† National Taiwan University.
‡ University of Frankfurt.

Table II. Atomic Fractional Coordinates and Thermal Parameters: (a) Full Data Refinement at 300 K; (b) Full Data Refinement at 104 K; (c) High-Order Refinement and Calculated H Atoms at 104 K

		x	y	z	B_{eq},[a] Å^2
S	a	0.207 60 (2)	0.096 00 (2)	0.061 50 (1)	1.91 (3)
	b	0.209 88 (2)	0.095 42 (2)	0.063 75 (1)	0.578 (3)
	c	0.209 87 (2)	0.095 40 (2)	0.063 78 (1)	0.566 (3)
C	a	0.108 00 (6)	−0.152 80 (6)	−0.068 20 (4)	2.1 (2)
	b	0.109 56 (8)	−0.156 78 (9)	−0.067 58 (6)	0.72 (1)
	c	0.109 66 (7)	−0.156 80 (7)	−0.067 52 (5)	0.715 (7)
O1	a	0.309 30 (4)	0.269 10 (4)	−0.030 50 (3)	3.1 (2)
	b	0.317 34 (8)	0.268 59 (7)	−0.029 44 (5)	1.03 (1)
	c	0.317 24 (7)	0.268 69 (7)	−0.029 54 (5)	1.028 (8)
O2	a	0.339 50 (4)	0.026 20 (4)	0.222 20 (3)	3.0 (1)
	b	0.341 44 (7)	0.025 93 (7)	0.227 92 (5)	0.984 (9)
	c	0.341 46 (7)	0.025 98 (7)	0.227 91 (4)	0.975 (7)
H1	a	0.826 00 (5)	0.287 00 (6)	0.013 00 (3)	2.4 (8)
	b	0.165 90 (2)	−0.296 40 (2)	−0.011 70 (1)	0.8 (2)
	c	0.834 00 (8)	0.296 00 (8)	0.012 00 (5)	0.8 (4)
H2	a	0.858 00 (5)	0.132 00 (4)	0.178 00 (4)	3.2 (8)
	b	0.146 80 (2)	−0.136 90 (2)	−0.173 70 (1)	1.6 (2)
	c	0.853 00 (7)	0.137 00 (7)	0.174 00 (5)	1.6 (4)

[a] $B_{eq} = {}^8/_3\pi^2\sum_i\sum_j U_{ij}\,\mathbf{a}_i^*\mathbf{a}_j^*\,\mathbf{a}_i\cdot\mathbf{a}_j$.

monitored reflections was found for the low-temperature measurements, and the scale of the relative intensities were corrected accordingly. An absorption correction according to seven measured faces was applied to the low-temperature data. All of the computations were carried out on a local PDP-8 computer using mainly NRCC programs[3] and locally developed programs for Fourier syntheses in an arbitary plane and the contour plotting.[4]

Results

Refinement. The parameters from the full data refinements at both temperatures, as well as from the high-order ($(\sin\theta)/\lambda > 0.65$) data refinement at 104 K are given in Table II. A few different $(\sin\theta)/\lambda$ cutoff values were tried in the least-squares refinement in order to obtain suitable atomic parameters for promolecule subtraction in deformation density studies shown below. The positional parameters do not change with the cutoff values. However the thermal parameters do change slightly. A value of 0.65 Å^{-1} was chosen based on the basis of the results of the refinement and its validity from the deformation density studies. The thermal ellipsoids of the molecule and the bond lengths at both temperatures are shown in Figure 1. Thermal parameters of the non-hydrogen atoms decreased to 30% on average by lowering the temperature from 300 to 104 K. However the anisotropy in thermal vibrations did not change significantly. The atomic scattering factors, f_o, are calculated on the basis of the analytical form, and the coefficients are taken from ref 5a f', f'' are taken from ref 5b.

Deformation Density Maps. The deformation density is a difference density representing the difference between the observed density, ρ_o, and the superposition of the sum of spherically averaged free atom densities, ρ_c. This difference density distribution describes the change in electron density associated with the formation of a molecule from the free atoms; i.e., they may be correlated directly to chemical bonding. The deformation density maps shown here were calculated up to a resolution of $(\sin\theta)/\lambda = 0.85$ Å^{-1}. The Fourier coefficients were taken to be the differences between the scaled measured scattering amplitude (kF_o) and F_c calculated by the parameters obtained from high-order ($(\sin\theta)/\lambda > 0.65$) refinement. Here k is the optimum scale factor for the data to be used in the Fourier calculation. Different resolution limits, namely 0.66, 0.85, 1.0, and 1.2, were also tried. The value of 0.85 was chosen because it gave the least level of noise but still maintained the important feature of the electron density distribution. The deformation electron density distributions for various planes of the molecule are illustrated in Figures 2–6. All the maps shown here are averaged over all chemically equivalent planes. (The estimate standard deviation at a general position in the deformation map is on the average 0.08 e Å^{-3}, and the differences between the individual density and the average density

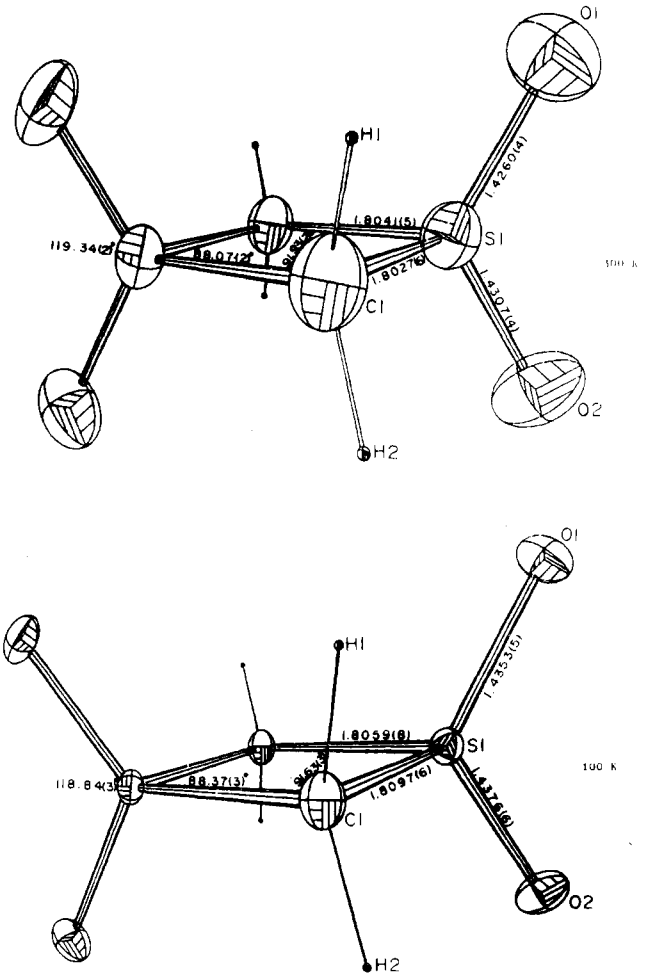

Figure 1. ORTEP drawings of thermal ellipsoids of 50% probability at both temperatures, hydrogen atom with fixed radii.

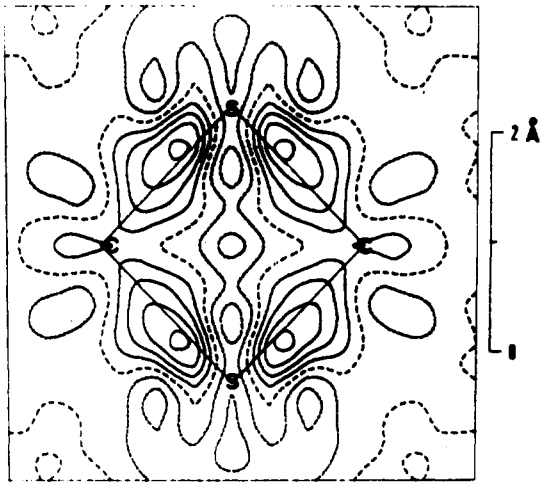

Figure 2. Deformation density map (D map) of the four-membered ring. Contour interval is 0.1 e Å^{-3} with the solid line as positive and the dotted line as zero and negative.

(1) Balbach, B.; Weichmann, K.; Ziegler, M. L. *Liebigs Ann. Chem.* **1980**, 1981.
(2) Opitz, G.; Mohl, H. R. *Angew. Chem., Int. Ed. Engl.* **1969**, *8*, 73.
(3) Larson, A. C.; Gabe, E. J. *Computing in Crystallography* Schenk, H., Ed.; Delft University Press: Delft, The Netherlands, 1978.
(4) Tsai, C. J. Master's Thesis, National Taiwan University, 1982.
(5) *International Tables for X-ray Crystallography*; Kynoch: Birmingham, England, 1974: (a) Vol. IV; (b) Vol. III, p 276.

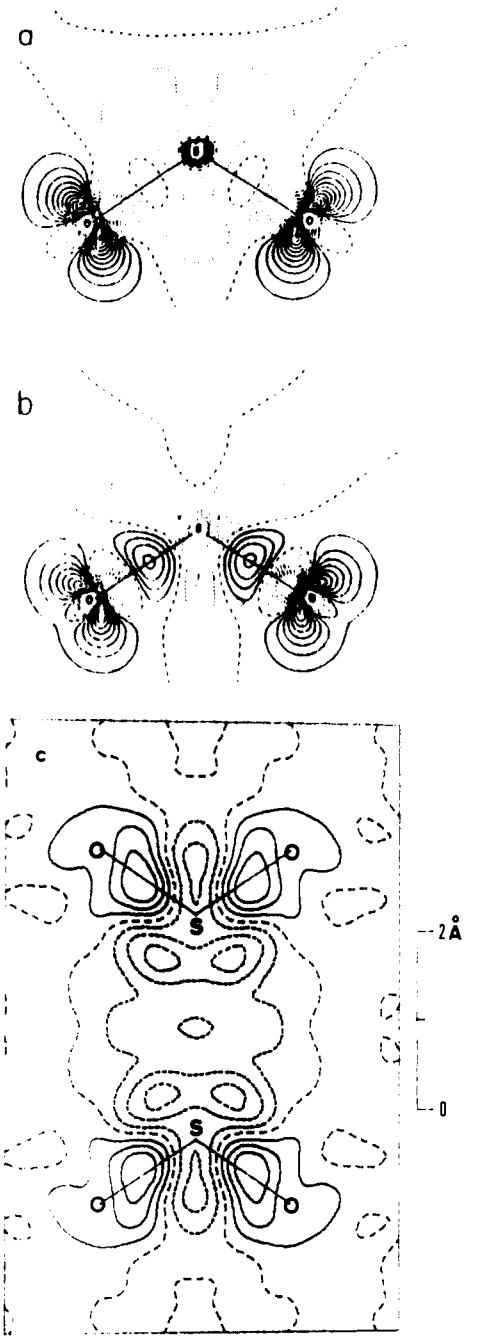

Figure 3. (a) Theoretical map of the SO_2 plane in H_3NSO_3 with a double-ζ basis set and no d function of the sulfur atom.[12] (b) Theoretical map of the SO_2 plane in H_3NSO_3 with a double-ζ basis set and d functions of the sulfur atom.[12] (c) *D* map of the SO_2 plane. Contours are as in Figure 2.

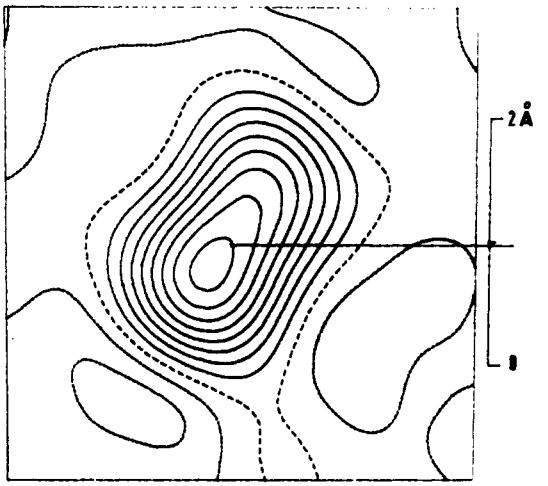

Figure 4. *D* map of the plane that is perpendicular to and bisects the S–O bond. The line indicates the projection of the other oxygen atom with a contour interval of 0.05 e Å^{-3}; others are as in Figure 2.

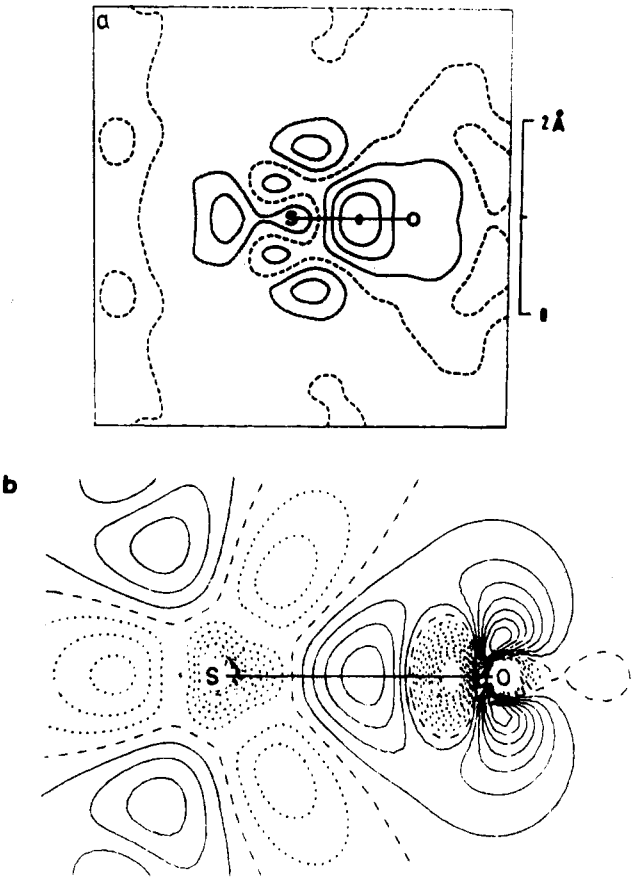

Figure 5. (a) *D* map of the plane that is perpendicular to and includes the S–O bond. (b) Theoretical map of curve a.[12] Contours are as in Figure 2.

are all within 2 esd.) Figure 2 shows the four-membered ring plane. There is positive density accumulation in the S–C bond, but peaking slightly outward from the ring edge and somewhat shifted toward the sulfur atom from the midpoint of S–C bonds. This shift occurred only when high-order reflections (>0.65 Å^{-1}) were included. The peak height in this map is 0.4 e Å^{-3}. Figure 3 depicts the plane of $-SO_2$, which is roughly perpendicular to the plane of that four-membered ring with a dihedral angle of 87.9°. Here we find bond electron density at the midpoint of the S–O bond. Figures 4 and 5 give the deformation density of the plane perpendicular to but bisecting the S–O bond and that perpendicular to but including the S–O bond, respectively. The elongation pattern in Figure 4 demonstrates the π-character of the bond. The lone-pair electron density of the oxygen atom can be seen in Figure 5. The $-CH_2$ plane is also roughly perpendicular to the four-membered ring (dihedral angle 94.2°). Bonding electron density accumulates as expected at the midpoint of the C–H bond as shown in Figure 6. This density is significantly enhanced (0.4 e Å^{-3} vs 0.1 e Å^{-3}) by displacing the H atom along the C–H vector (obtained from least-squares refinement) to yield a distance of 1.08 Å for the C–H bond.[5b] The deformation density maps in this work are therefore calculated with such adjusted hydrogen positions.

Discussion

Although the molecular site symmetry in the crystal is only C_i, it shows no significant deviations from D_{2h}. The molecule is assumed to be D_{2h} after the averaging over the chemical equivalents in the deformation density distribution. The density distribution of chemical equivalent planes do appear similar before averaging. From the deformation density map shown above, the

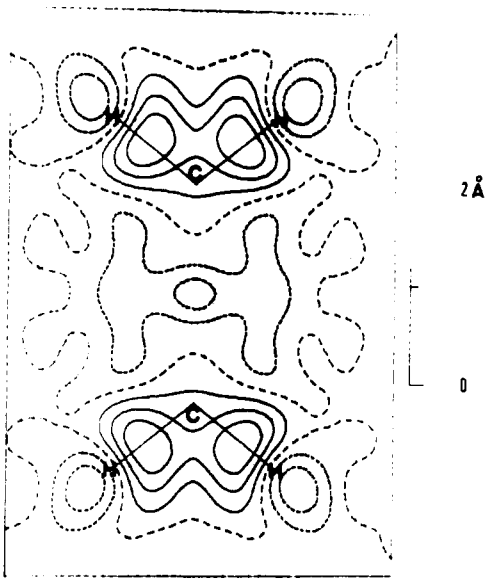

Figure 6. *D* map of the CH_2 plane. Contours are as in Figure 2.

four-membered ring formed by two sulfur atoms and two carbon atoms does show evidence of the ring strain (Figure 2), though not as much as that of cyclobutadiene derivatives.[6] The two S–C bond density maxima make a 105° angle at the sulfur atom, whereas the C–S–C angle is only 88.07 (2)°. The corresponding angles in cyclobutadiene derivatives are 115 and 90°.[6] The displacement of the density maximum toward the sulfur atom seems to be contributed mainly from high-order reflections; the deformation density calculated with data of $(\sin\theta)/\lambda$ up to 0.65 $Å^{-1}$ does not give such displacement. The reason for such displacement is unclear. However in other experimental density studies,[7] the lone-pair electron region seems to be enhanced also by including higher order reflections.

The SO_2 group is nearly perpendicular to the plane of four-membered ring. The O–S–O angle of the SO_2 group in the molecule is 118.84 (3)°, which is larger than that of SO_3^- (~115°) in various structures[8-10] but close to that of the sulfonyl group[11] and the SO_2 molecule. The deformation density map in the $-SO_2$ plane shown in Figure 3 illustrates a well-characterized S–O bond, which is quite similar to that of the theoretical map[12] for H_3NSO_3 obtained from an ab initio calculation with a double-ζ basis set including d functions of the sulfur atom (Figure 3b). Apparently the d functions of the sulfur atom in the polarization basis set are very important for S–O electron density accumulation. According to the calculation,[12] the basis set without the d functions of the sulfur atom gave practically no accumulation of density at the midpoint of the S–O bond (Figure 3a). Thus our experimental results (Figure 3c) confirm that the d functions of sulfur atom in the polarization basis sets are important for the theoretical bonding electron density studies (Figure 3b). The π-character of the S–O bond can be demonstrated by elongation of the density in the perpendicular plane bisecting the bond (Figure 4). Another perpendicular plane including the S–O bond (Figure 5a) shows good agreement with that (Figure 5b) of theoretical map[12] in the S–O bond. However, the high positive peaks in the lone-pair region and a big negative hole along the O–S bond near the oxygen atom in the theoretical map are not so well reproduced in the experimental map. Such phenomena were known[13,14] previously in many experimental results. The most probable explanation of such disagreement is the limitation of the diffraction data measured in the experimental map and the lack of thermal smearing in the theoretical calculation.

The hydrogen atom positions were known[15] to be affected by the bonding electron density to yield somewhat shorter interatomic distances with the X-ray diffraction method. The lengthening of C–H bond length to a recognized true value[5] (1.08 Å) is an attempt to eliminate the biased results in the C–H bonding region. The bond electron density of the C–H bond (Figure 6) was indeed enhanced significantly by doing so.

There is a short S–S distance of 2.593 Å, which is much shorter than the sum of the van der Waals radii and is only slightly longer than some sulfur–sulfur single bond distances, e.g. 2.5087 (4) Å in thiathiophthene[16] and 2.48 Å in $Na_2S_2O_4$.[17] In this deformation density study, it is apparent that there is no accumulation of density in the S–S internuclear region (Figure 3); instead there is a depletion of density compared with the sum of independent spherical atoms. Bonding electron density deficits have been found in various deformation density studies along OO, NN, and CF bonds.[18-20] Quite a few theoretical discussions[21-23] on the various models of "oriented atoms" or "valence state of the hybrid atoms" in the promolecule have been proposed in order to understand the correlation between the density deficits and the concept of covalent bonding for electron-rich atoms. The deficit density along the sulfur–sulfur direction across the ring may be interpreted in the same way. However, it is hard to conclude whether there is a sulfur–sulfur interaction across the ring until some theoretical calculations are carried out.

Conclusion

By comparison of the experimental deformation density maps with theoretical calculated ones, it is confirmed that the d functions of sulfur atom do play an important role on the density accumulation in the S–O bonds of this compound. However the S–S interaction can not be determined. It may be concerned with whether the sulfur atomic state is spherical or not in the promolecule.

Acknowledgment. We wish to thank the National Science Council of the Republic of China for financial support.

Registry No. $(CH_2SO_2)_2$, 21511-46-6.

Supplementary Material Available: Tables SI and SII listing anisotropic temperature factors and hydrogen atom coordinates and isotropic thermal parameters (1 page); tables of calculated and observed structure factors (22 pages). Ordering information is given on any current masthead page.

(6) Irngartinger, H. *Electron Distribution and Chemical Bonding*; Coppens, P., Hall, M. B., Eds.; Plenum: New York, 1982; p 361.
(7) Wang, Y.; Blessing, R. H.; Ross, F.; Coppens, P. *Acta Crystallogr., Sect. B: Struct. Crystallogr. Cryst. Chem.* **1976**, *B32*, 572.
(8) Bats, J. W.; Coppens, P.; Koetzle, T. F. *Acta Crystallogr., Sect. B: Crystallogr. Cryst. Chem.* **1977**, *B33*, 1304.
(9) Kirfel, A.; Will, G. *Acta Crystallogr., Sect. B: Struct. Crystallogr. Cryst. Chem.* **1980**, *B36*, 512.
(10) Chen, I.; Wang, Y. *Acta Crystallogr., Sect. C.: Cryst. Struct. Commun.* **1984**, *C40*, 1780.
(11) Chen, I.; Wang, Y. *Acta Crystallogr., Sect. C.: Cryst. Struct. Commun.* **1984**, *C40*, 1890.
(12) Cruickshank, D. W. J.; Eisenstein, M. *J. Mol. Struct.* **1985**, *130*, 143.
(13) Wang, Y.; Angermund, K.; Goddard, R.; Kruger, C. *J. Am. Chem. Soc.* **1987**, *109*, 587.
(14) Angermund, K.; Claus, K. H.; Goddard, R.; Kruger, C. *Angew. Chem.* **1985**, *97*, 241; *Angew. Chem., Int. Ed. Engl.* **1985**, *24*, 237.
(15) Coppens, P.; Dam, J.; Harkema, S.; Feil, D.; Feld, R.; Lehmann, M. S.; Goddard, R.; Kruger, C.; Hellner, E.; Johansen, H.; Larsen, F. K.; Koetzle, T. F.; McMullan, R. K.; Maslen, E. N.; Stevens, E. D. *Acta Crystallogr., Sect. A: Found. Crystallogr.* **1984**, *A40*, 184.
(16) Wang, Y.; Chen, M. J.; Wu, C. H. *Acta Crystallogr., Sect. B: Struct. Sci.*, in press.
(17) Dunitz, J. D. *Acta Crystallogr.* **1956**, *9*, 579.
(18) Savariault, J. M.; Lehmann, M. S. *J. Am. Chem. Soc.* **1980**, *102*, 1298.
(19) Dunitz, J. D.; Seiler, P. *J. Am. Chem. Soc.* **1983**, *105*, 7056.
(20) Dunity, J. D.; Schweizer, W. B.; Seiler, P. *Helv. Chim. Acta* **1983**, *66*, 123.
(21) Kunze, K. L.; Hall, M. B. *J. Am. Chem. Soc.* **1986**, *108*, 5122.
(22) Kutzelnigg, K., *Angew. Chem., Int. Ed. Engl.* **1984**, *23*, 272.
(23) Schwarz, W. H. E.; Valtazanos, P.; Ruedenberg, K. *Theor. Chim. Acta* **1985**, *68*, 471.